ZIBELINE INTERNATIONAL™ PUBLISHING

ISSN: 2521-0912 (Print)
ISSN: 2521-0513 (Online)
CODEN: JCOLBF

Journal Clean WAS (JCleanWAS)

DOI: http://doi.org/10.26480/jcleanwas.01.2021.27.30

RESEARCH ARTICLE

FACILE FABRICATION OF COPPER OXIDE NANOPARTICLES FOR ANTIMICROBIAL ACTIVITY

Md. Ashraful Haque, Md. Kaium Hossain, Md. Ashraful Islam Molla, Mithun Sarker, Shaikat Chandra Dey, Md. Ashaduzzaman*

Department of Applied Chemistry and Chemical Engineering, Faculty of Engineering and Technology, University of Dhaka, Dhaka 1000, Bangladesh
Corresponding Author Email: azaman01@du.ac.bd

ARTICLE DETAILS

Article History:

Received 02 April 2021
Accepted 06 May 2021
Available online 09 June 2021

ABSTRACT

Copper Oxide nanoparticles (NPs) have shown great acceptance in the antimicrobial application owing to their low toxicity and high surface to charge ratio. In this study, copper oxide NPs (represented as S-1, S-2 and S-3) were prepared by a simple and cost-effective thermal approach in three different environments. Fabricated NPs were characterized using x-ray diffraction (XRD), scanning electron microscopy (SEM), ultraviolet-visible (UV-Vis) spectroscopy and Fourier transform infrared spectroscopy (FTIR) technique. The XRD patterns revealed that the synthesized S-2 was of pure Cu_2O phase while S-3 was composed of monoclinic CuO with a small quantity of Cu_2O. More importantly, synthesized copper oxide NPs were used to evaluate the antimicrobial activity against three types of gram-negative bacteria namely *Salmonella typhi*, *SK4* and *E. coli* (two strains). Although the NPs produced from the S-1 approach did not show encouraging results, the copper oxide NPs from S-2 and S-3 had shown enhanced antimicrobial activity. The successful antimicrobial activity of S-2 and S-3 can be related to the release of Cu^{+} and Cu^{2+} ions into the surrounding environment, which is responsible for the breaking of the cell wall membrane and ultimately causes bacterial cell disruption. The synthesized copper oxide NPs via thermal approach will be good candidates for biomedical applications.

KEYWORDS

Antimicrobial activity, Copper oxide, Nanoparticles, Thermal approach.

1. INTRODUCTION

In today's world, nanometer-sized metal oxides (MOs) have a great impact on several aspects (Hu et al., 2015; Dehhaghi et al., 2019). Recently, considerable efforts have been made to characterize and describe the physical and chemical properties of MO nanoparticles (NPs) because of their significant applications in numerous technological fields (Ahmed et al., 2020; Xu et al., 2012). The oxides of transition metals are important class of semiconductors that have wider applications in the field of electronics, biological and catalytic reactions (Wojcieszak et al., 2014; Sahmani et al., 2019). Copper oxides have been a hot topic among the studies on transition MOs because of their interesting properties as a p-type semiconductor with a narrow band gap (Zhang et al., 2014). Copper oxide NPs are extensively used in various applications, including gas sensors, bio-sensors, photodetectors, supercapacitors, photocatalysts, magnetic storage media and especially antimicrobial agents (Zhang et al., 2014; Tran and Nguyen, 2014).

Various techniques (Zhang et al., 2014; Tran and Nguyen, 2014; Suleiman et al., 2013) such as thermal decomposition, microwave irradiation, sol-gel, chemical precipitation and electrochemical methods are practiced for the preparations of copper oxide NPs. Among them, thermal decomposition method is considered very promising due to facile synthesis and low cost (Al-Gaashani et al., 2011; Bakhtiari and Darezereshki, 2011). Vellora et al. (2013) prepared CuO NPs through the green synthesis technique and studied the antibacterial inhibition zone towards *E.coli*. George et al. (2020) investigated the effect of calcination temperature on the CuO nanostructures and reported that the prepared CuO nanostructures possessed better antibacterial properties for gram-negative bacterial strains. Contrarily, Bhosale and Bhanage (2016) fabricated Cu_2O NPs by sonochemical synthesis and applied for electrocatalytic application. In addition, Mikami et al. (2019) synthesized Cu_2O/CuO nanocrystals and applied for H_2S sensing. Recently, Khalaji et al. (2020) prepared copper oxide nanocomposites as antimicrobial agents. Therefore, synthesis of copper oxide NPs with both Cu_2O and CuO phase are very attractive considering its excellent antimicrobial activity.

Herein, the thermal decomposition method was followed to synthesize copper oxide NPs using different matrices such as urea and ash to investigate the variation in size and morphology of the synthesized NPs. The synthesized copper oxide NPs showed different antimicrobial properties depending on the size. Moreover, plausible mechanisms for antimicrobial activity using copper oxide NPs are suggested.

2. MATERIALS AND METHODS

2.1 Chemicals

Copper nitrate trihydrate ($Cu(NO_3)_2.3H_2O$) was purchased from Loba

Quick Response Code	Access this article online	
	Website: www.jcleanwas.com	DOI: 10.26480/jcleanwas.01.2021.27.30

Cite the Article: Md. Ashraful Haque, Md. Kaium Hossain, Md. Ashraful Islam Molla, Mithun Sarker, Shaikat Chandra Dey, Md. Ashaduzzaman (2021). Facile Fabrication of Copper Oxide Nanoparticles for Antimicrobial Activity. *Journal Clean WAS, 5(1): 27-30*.

Chemicals, India and used to produce copper oxide NPs. Granular urea (NH_2CONH_2) was collected from the local market. Trash offset paper from the bin was used to produce ash. Hydrochloric acid (HCl) was purchased from Merck, India and used to wash the product. Deionized water was used for the preparation of solutions.

2.2 Synthesis of copper oxide NPs

For the first approach (Figure 1a), 1 gm Cu $(NO_3)_2.3H_2O$) salt was taken and ground in mortar and pestle. Then the salt was kept in crucible and heat-treated in a muffle furnace for 2 hours at a temperature of 350 °C. Thermal decomposition of Cu $(NO_3)_2.3H_2O$) occurred during this treatment and the prepared product was prescribed as S-1.

In the second approach (Figure 1b), urea (NH_2CONH_2) and Cu $(NO_3)_2.3H_2O$) were taken as 1:1 weight ratio in the mortar and finely ground into a homogeneous mixture. The mixture was then heat-treated in a muffle furnace for 2 hours at a temperature of 350 °C. The prepared copper oxide was washed with deionized water properly for purification and then dried in a dryer at 100 °C for 1 hour. The synthesized product was identified as S-2.

For the third approach (Figure 1c), the paper was burned and heat-treated in a muffle furnace at 500 °C for half an hour. Paper ash and Cu $(NO_3)_2.3H_2O$) were then mixed thoroughly in 1:1 weight ratio and ground using mortar and pestle. Then, the mixture was heat-treated in a muffle furnace for 2 hours at a temperature of 350 °C. The prepared product was washed with 0.5 M HCl to remove the ash. The copper oxide NPs was washed with water and dried at 100 °C for 1 hour at atmospheric drier and the product was named S-3.

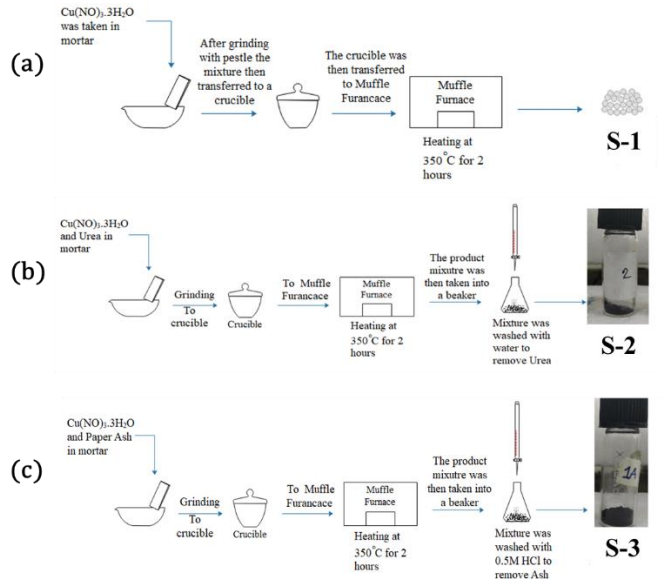

Figure 1: Copper oxide NPs produced (a) without any matrix, (b) using urea as a matrix and (c) using ash as a matrix.

2.3 Characterizations

X-ray diffraction (XRD) was used to investigate the cell dimensions and phase identification of copper oxide NPs. The XRD patterns of the samples were recorded by an x-ray diffractometer (Ultima IV, Rigaku Corporation, Japan). Cu Kα radiation was applied to the samples at 40 kV and 40 mA. The morphological feature of the copper oxide NPs were studied using a JEOL 6400 SEM at an accelerating voltage of 25 kV. The SEM specimens were sputter-coated with platinum. The synthesized copper oxide NPs were monitored using UV-Vis spectrophotometer UV-2100PC (Human Lab Instrument Co., Korea) between the range of 200-800 nm. The infrared spectra for the synthesized copper oxide NPs were recorded for the identification of functional groups in a FTIR 8400S spectrophotometer (Shimadzu Co. Japan) by employing the KBr pellet technique and registering amplitude waves ranging from 450 to 4000 cm^{-1}.

2.4 Determination of antimicrobial activity

Six isolates were subjected to antimicrobial sensitivity tests using the agar well diffusion method. Two types of concentration were used: 5 mg/mL and 20 mg/mL. All of them were dissolved in distilled water and subjected to sonication for 10 mins. A spectrophotometer was used to adjust the OD (0.1-0.5) *E. coli* for reference strains. At least four well-isolated colonies of the same type from a culture agar plate were selected and touched the top of the colony with a loop and transferred to a tube containing 5 mL of a Mueller Hinton broth. The suspension was incubated at 37 °C and the size was adjusted to the OD 0.1-0.5. Two types of concentrations were used: 5 mg/mL and 20 mg/mL. All of them were dissolved into distilled water and subjected to sonication for 10 min. Ampicillin was used as a control for the microorganism's assay. Firstly, homogeneous bacterial lawn was prepared using a sterile cotton swab and made the well with the bits of the help of serial corks borer. Each well was filled with 40 µL diluted samples and incubated at 37 °C for 24 hours.

3. Results and Discussion

The properties of the copper oxide NPs depend solely on the synthesis method selected. The synthesis technique is important since it may control the size and morphology of the NPs. Copper oxide NPs prepared by using the thermal technique can improve properties which may be helpful in their biomedical applications (George et al. 2020).

3.1 XRD study

The powder XRD patterns of synthesized copper oxide NPs together with the simulated pattern of Cu_2O and CuO are shown in Figure 2. The XRD patterns of S-2 are nicely matched with the simulated pattern of the Cu_2O phase (JCPDF No., 01-0801916) (Rashmi et al., 2020; Meghana et al., 2015). While the synthesized S-3 is composed of a monoclinic CuO phase with a small quantity of cubic fcc structure of Cu_2O (JCPDF No., 05-0667) (Meghana et al., 2015). However, the XRD pattern of S-1 neither matched with the monoclinic CuO nor cubic fcc structure of Cu_2O. The reflections observed for copper oxide NPs (S-2 and S-3) and simulated CuO at 2θ values of 32.4°, 35.4°, 38.7°, 48.8°, 53.4°, and 58.1° are the typical characteristic peaks of monoclinic crystalline CuO and their matching (hkl) planes are (110), (111), (111), (200), (020) and (202), respectively (Gopinath et al., 2016; Siddiqui et al., 2018). Moreover, the characteristic peak observed for S-3 at 2θ ~ 29.4° indicates the (110) plane of the cubic structure of Cu_2O (Gopinath et al., 2016). The particle size of copper oxide NPs (S-2 and S-3) were calculated by the Debye-Scherrer equation (Sarker et al., 2019) using the full width at half maximum (FWHM) of the X-ray diffraction peak at 2θ ~35.4° corresponding to the most intense peak of monoclinic CuO (Siddiqui et al., 2018). According to the Debye-Scherrer equation, the particle size of S-2 and S-3 were 26.1 and 27.8 nm respectively.

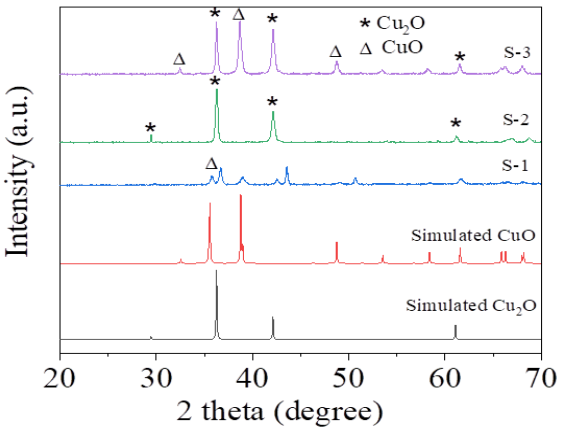

Figure 2: XRD patterns of copper oxide NPs produced by three different approaches.

3.2 SEM study

The SEM images of copper oxide NPs produced from different thermal approaches are presented in Figure 3. As shown in Figure 3a, S-1 is irregular structures and has a high degree of agglomeration. The surface of S-2 is relatively smooth and they are spherical in shapes (Figure 3b) (Altikatoglu et al., 2017). The S-3 shows flake shape NPs as depicted in Figure 3c (Siebert et al., 2015). The average size of the copper oxide NPs observed by SEM is in the nanometer range, which is consistent with the XRD results.

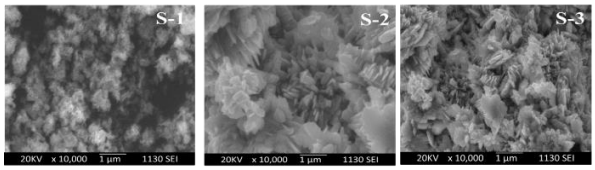

Figure 3: SEM images of copper oxide NPs (a) S-1 (b) S-2 and (c) S-3.

3.3 UV-visible spectra study

Ultraviolet and visible (UV-Vis) absorption spectroscopy is the measurement of the attenuation of a beam of light after it passes through a sample or after reflection from a sample surface. Absorption measurement can be a single wavelength or over an extended spectral range. For copper oxide NPs the analysis was done in the range of 200-400 nm. The three different copper oxide NPs showed absorption peak around 280-300 nm (Figure 4) which is correlated with external standards (Tadjarodi et al., 2014).

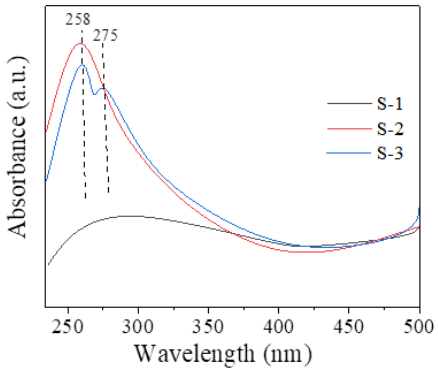

Figure 4: UV-Vis absorption spectra of copper oxide NPs produced by three different approaches.

3.4 FTIR analysis

FTIR transmission spectra of copper oxide NPs are were recorded and shown in Figure 5. The broad absorption peaks at around 3435 to 3440 cm^{-1} are caused by the adsorbed water molecules which suggest that the NPs possess a high surface to volume ratio (Altanany et al., 2018). The absorption band near 1130 cm^{-1} corresponds to the stretching vibration of the Cu–O bond of copper (I) oxide NPs (Lai et al., 2015). Moreover, sharp peaks at 798 cm^{-1} and 628 cm^{-1} are ascribed to Cu_2O stretching mode, which is observed in S-2 and S-3 of Figure 5 (Lai et al., 2015; Sahai et al., 2016). However, other IR active modes at 535 cm^{-1} and 482 cm^{-1} were detected in S-3, which indicates the existence of CuO (Sahai et al., 2016). Thus, the pure phase of Cu_2O was formed only in S-2 whereas mixed phases Cu_2O and CuO existed in S-3 as confirmed from the FTIR analysis.

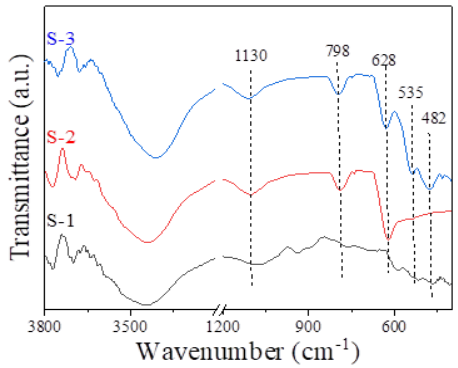

Figure 5: FTIR spectra of copper oxide NPs produced by three different approaches.

3.5. Antimicrobial activity

The copper oxide NPs were used to evaluate the antimicrobial activity against four gram-negative bacteria of *Salmonella typhi*, *SK4*, *E. coli RN89* and *E. coli DH5α*. The zone of inhibition (ZOI) study for the four-gram negative bacteria with S-1 showed no activity against any of the bacteria as displayed in Table 1. This is because S-1 neither forms CuO nor cubic fcc structure of Cu_2O. The antimicrobial activity of copper oxide NPs is very much dependent on particle size (Applerot et al., 2012). The cell membrane contains numerous nanometer-sized pores and the high amount of agglomeration in S-1 makes it unable to enter and penetrate the cell wall of different types of bacteria (Meghana et al., 2015). The NPs of Cu_2O (S-2) showed a significant ZOI against *Salmonella typhi*, *SK4*, *E. coli RN89* and *E. coli DH5α* (Table 1). This is due to the release of Cu^+ ions into the surrounding medium which leads to the breaking and disruption of the cell wall membrane effectively as shown in Figure 6 (Meghana et al., 2015).

Table 1: Diameter of inhibition zone of copper oxide NPs against *Salmonella typhi, SK4, E. coli RN89* and *E. coli DH5α.*

Copper oxide NPs	Concentration (mg/mL)	Inhibition zone (mm)			
		Salmonella typhi	*SK4*	*E. coli RN89*	*E. coli DH5α*
S-1	5	R	R	R	R
	20	R	R	R	R
S-2	5	7	6	8	9
	20	11	10	12	14
S-3	5	7	7	9	10
	20	12	14	15	17

The highest antibacterial activity has been observed for the S-3 as presented in Table 1. S-3 is composed of a monoclinic CuO phase with a small quantity of cubic fcc structure of Cu_2O. The monoclinic CuO release Cu^{2+} ions into the surrounding environment changes the charge of the surrounding medium which allows the membrane damage of bacterial cells. These Cu^{2+} ions disrupt the biochemical processes that undergo inside the bacterial cells leading to bacterial death (George et al., 2020). Moreover, the combination of CuO phase and Cu_2O in S-3 increases the ZOI remarkably (Nieto-Juarez et al., 2010). Thus, the productions of reactive oxygen species (ROS), protein denaturation, cell membrane damage, DNA damage are responsible for the death of the bacteria strains (Qamar et al., 2020). The plausible mechanisms of antibacterial activity of produced copper oxide NPs (S-1, S-2 and S-3) are described in Figure 6.

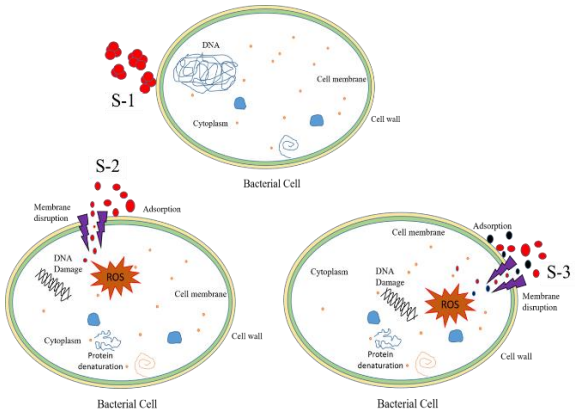

Figure 6: Plausible mechanism of antibacterial activity of produced copper oxide NPs.

4. Conclusion

The successful synthesis of copper oxide NPs through thermal approaches was carried out in this study. The XRD analysis confirmed that the NPs are crystalline, and the size of those NPs was in the nanometer range. The SEM image of the NPs established the formation of spherical shapes for S-2 and flake shapes for S-3. The optical property and the FTIR analysis were also performed to confirm the successful synthesis of NPs. It is observed that the NPs made from three different approaches have different antibacterial activity. Among them, S-3 showed the best result because it was composed of a monoclinic CuO phase with a cubic fcc structure of Cu_2O. Thus the prepared copper oxide NPs are potential candidates for antimicrobial application.

Acknowledgments

The authors are grateful to the Centre for Advanced Research in Sciences (CARS), University of Dhaka, Dhaka 1000, Bangladesh for providing analytical facilities for characterizing the products.

REFERENCES

Ahmed, A.Z., Islam, M.M., Islam, M.M.-ul., Masum, S.M., Islam, R., Molla, M.A.I., 2020. Fabrication and characterization of B/Sn-doped ZnO nanoparticles via mechanochemical method for photocatalytic degradation of rhodamine B. Inorganic and Nano-Metal Chemistry, DOI: 10.1080/24701556.2020.1835976.

Al-Gaashani, R., Radiman, S., Tabet, N., Daud A.R., 2011. Synthesis and optical properties of CuO nanostructures obtained via a novel thermal decomposition method. Journal of Alloys and Compounds, 509, Pp. 8761–8769.

Altanany, S.M., Gondal, M.A., Baig, U., 2018. Synthesis and characterization of CuO/WO_3 nanocomposite using hybrid method: Simple precipitation and pulsed laser ablation in liquids technique. AIP Conference Proceedings, 1976 (1), Pp. 020014.

Altikatoglu, M., Attar, A., Erci, F., Cristatache, C., Isildak, I., 2017. Green synthesis of copper oxide nanoparticles using Ocimum basilicum extract and their antibacterial activity. Fresenius Environmental Bulletin, 26(12A), Pp. 7832–7837.

Applerot, G., Lellouche, J., Lipovsky, A., Nitzan, Y., Lubart, R., Gedanken, A., Banin, E, 2012. Understanding the antibacterial mechanism of CuO nanoparticles: revealing the route of induced oxidative stress. Small, 8, Pp. 3326–3337.

Bakhtiari, F., Darezereshki, E., 2011. One-step synthesis of tenorite (CuO) nano-particles from Cu_4 (SO_4) $(OH)_6$ by direct thermal-decomposition method. Materials Letters 65, Pp. 171–174.

Bhosale, M.A., Bhanage, B.M., 2016. A simple approach for sonochemical synthesis of Cu_2O nanoparticles with high catalytic properties. Advanced Powder Technology, 27, Pp. 238–244.

Darezereshki, E., Bakhtiari, F., 2011. A novel technique to synthesis of tenorite (CuO) nanoparticles from low concentration $CuSO_4$ solution. Journal of Mining and Metallurgy Section B Metallurgy, 47 (1), Pp. 73–78.

Dehhaghi, M., Meisam, T., Aghbashlo, M., Panahi, H.K.S., Nizami, A.-S., 2019. A state-of-the-art review on the application of nanomaterials for enhancing biogas production. Journal of Environmental Management, 251, Pp. 109597.

George, A., Raj, D.M.A., Raj, A.D., Irudayaraj, A.A., Arumugam, J., Kumar, M.S., Prabu, H.J., Sundaram, S.J., Al-Dhabi, N.A., Arasu, M.V., Maaza, M., Kaviyarasu, K., 2020. Temperature effect on CuO nanoparticles: Antimicrobial activity towards bacterial strains. Surfaces and Interfaces, 21, Pp. 100761.

Gopinath, V., Priyadarshini, S., Al-Maleki, A.R., Alagiri, M., Yahya, R., Saravanan, S., Vadivelu, J., 2016. In vitro toxicity, apoptosis and antimicrobial effects of phyto-mediated copper oxide nanoparticles. RSC Advances, 6, Pp. 110986–110995.

Hu, B., He, M., Chen, B., 2015. Nanometer-sized materials for solid-phase extraction of trace elements, Analytical and Bioanalytical Chemistry, 407, Pp. 2685–2710.

Khalaji, A.D., Jarosova, M., Machek, P., 2020. The preparation, structural characterization, optical properties, and antibacterial activity of the CuO/Cu_2O nanocomposites prepared by the facile thermal decomposition of a new copper precursor. Nanomedicine Journal, 7(3), Pp. 231–236.

Lai, D., Liu, T., Gu, X., Chen, Y., Niu, J., Yi, L., Chen, W., 2015. Suspension synthesis of surfactant-free cuprous oxide quantum dots. Journal of Nanomaterials, 2015, Pp. 1–8.

Meghana, S., Kabra, P., Chakraborty, S., Padmavathy, N., 2015. Understanding the pathway of antibacterial activity of copper oxide nanoparticles. RSC Advances, 5, 12293–12299.

Mikami, K., Kido, Y., Akaishi, Y., Quitain, A., Kida, T., 2019. Synthesis of Cu_2O/CuO Nanocrystals and Their Application to H_2S Sensing. Sensors, 19(1), Pp. 211

Nieto-Juarez, J. I., Pierzchła, K., Sienkiewicz, A., Kohn, T., 2010. Inactivation of MS2 coliphage in Fenton and Fenton-like systems: role of transition metals, hydrogen peroxide and sunlight. Environmental science & technology, 44, Pp. 3351–3356.

Qamar, H., Rehman, S., Chauhan, D.K., Tiwari, A.K., Upmanyu, V., 2020. Green synthesis, characterization and antimicrobial activity of copper oxide nanomaterial derived from momordica charantia. International Journal of Nanomedicine, 15, Pp. 2541.

Rashmi, M., Padmanaban, R., Vaithinathan, K., Roy, V.A.L., Gopalan, A.-I., Gopalan, S., Kim, W.-J., Kannan, V., 2020. A Comparative evaluation of physicochemical properties and photocatalytic efficiencies of cerium oxide and copper oxide nanofluids. Catalysts, 10 (1), Pp. 34.

Sahai, A., Goswami, N., Kaushik, S.D., Tripathi, S., 2016. $Cu/Cu_2O/CuO$ Nanoparticles: novel synthesis by exploding wire technique and extensive characterization. Applied Surface Science, 390, Pp. 974–983.

Sahmani, S., Shahali, M., Ghadiri Nejad, M., Khandan, A., Aghdam, M.M., Saber-Samandari, S., 2019. Effect of copper oxide nanoparticles on electrical conductivity and cell viability of calcium phosphate scaffolds with improved mechanical strength for bone tissue engineering. The European Physical Journal Plus, 134 (1), Pp. 7.

Sarker, M., Bhadra, B.N., Shin, S., Jhung, S.H., 2019. TiO_2-integrated carbon prepared via pyrolysis of Ti-loaded metal–organic frameworks for redox catalysis. ACS Applied Nano Materials, 2, Pp. 191–201.

Siddiqui, H., Parra, M.R., Qureshi, M.S., Malik, M.M., Haque, F.Z., 2018. Studies of structural, optical, and electrical properties associated with defects in sodium-doped copper oxide (CuO/Na) nanostructures. Journal of Materials Science, 53, Pp. 8826–8843.

Siebert, E., Laherisheth, Z., Upadhyay, R.V., 2015. Dilution dependent magnetorheological effect of flake-shaped particle suspensions–destructive friction effects. Smart Materials and Structures, 24 (7), Pp. 075011.

Suleiman, M., Mousa, M., Hussein, A., Hammouti, B., Hadda, T.B., Warad, I., 2013. Copper (II)-oxide nanostructures: synthesis, characterizations and their applications-review. Journal of Materials and Environmental Science, 4 (5), Pp. 792–797.

Tadjarodi, A., Roshani, R., 2014. A green synthesis of copper oxide nanoparticles by mechanochemical method. Current Chemistry Letters, 3 (4), Pp. 215–220.

Tran, T.H., Nguyen, V.T., 2014. Copper oxide nanomaterials prepared by solution methods, some properties, and potential applications: a brief review. International Scholarly Research Notices, 2014, Pp. 856592.

Vellora, V., Padil, T., Černík, M., 2013. Green synthesis of copper oxide nanoparticles using gum karaya as a biotemplate and their antibacterial application. International Journal of Nanomedicine, 8, Pp. 889–898.

Wojcieszak, D., Mazur, M., Kurnatowska, M., Kaczmarek, D., Domaradzki, J., Kepinski, L., Chojnacki, K., 2014. Influence of Nd-doping on photocatalytic properties of TiO_2 nanoparticles and thin film coatings. International Journal of Photoenergy, 2014, Pp. 463034.

Xu, X., Xu, C., Dai, J., Hu, J., Li, F., Zhang, S., 2012. Size dependence of defect-induced room temperature ferromagnetism in undoped ZnO nanoparticles. The Journal of Physical Chemistry C, 116, Pp. 8813–8818.

Zhang, Q., Zhang, K., Xu, D., Yang, G., Huang, H., Nie, F., Liu, C., Yang, S., 2014. CuO nanostructures: synthesis, characterization, growth mechanisms, fundamental properties, and applications. Progress in Materials Science, 60, Pp. 208–337.